Enzyme and Microbial Technology 154 (2022) 109959

Contents lists available at ScienceDirect

Enzyme and Microbial Technology

journal homepage: www.elsevier.com/locate/enzmictec

Immobilization of bovine hemoglobin on Au nanoparticles/MoS_2 nanosheets – Chitosan modified screen-printed electrode as chlorpyrifos biosensor

Wei Li [a], Zuyi Zhao [a], Wei Yang [a], Qin Su [a], Chong Na [b], Xueli Zhang [a], Rui Zhao [a], Haiyan Song [a,*]

[a] College of Agricultural Engineering, Shanxi Agricultural University, Taigu, Shanxi 030801, China
[b] Shanxi Wanjiazhai Water Resources Co., Ltd., Xinzhou, Shanxi 030012, China

ARTICLE INFO

Keywords:
Bovine hemoglobin
Electrochemical biosensor
Chlorpyrifos
Square wave voltammetry
Au nanoparticles

ABSTRACT

In this paper a quick and disposable electrochemical biosensor based on bovine hemoglobin (BHb) is proposed for the determination of chlorpyrifos (CP). The bioelectrode (denoted as AuNPs/MoS_2-CS/BHb/SPE) has been designed by immobilizing BHb on the screen printed electrode (SPE) surface modified by gold nanoparticles (AuNPs) and Molybdenum disulfide (MoS_2) nanosheets - chitosan (CS) mixture (MoS_2-CS). Field emission scanning electron microscopy (FESEM) and electrochemical characterization demonstrate the successful grafting of AuNPs/MoS_2-CS/BHb/SPE. Detailed electrochemical impedance spectroscopy (EIS) analysis and cyclic voltammetry (CV) tests show that the proposed bioelectrode exhibits decent electrochemical properties, such as well conductivity and large specific surface area. In-depth electrochemical analysis reveals the redox reaction occurring on the surface of the bioelectrode and the mechanism that CP binds with BHb forming the thin film to inhibit the peak current. The proposed biosensor exhibits sensitive and stable responses for electrochemical assay of CP ranging from 0.004 μM to 28.52 μM, with a limit of detection (LOD) as 5.6 nM. The electrochemical biosensor passes the repeatability, reproducibility, stability and anti-interference ability test experiments with good performance. The biosensor also shows its credibility for detecting CP in real vegetable samples (Cabbage and Leek) with recovery (%) ranging from 87% to 109%. The proposed biosensor is of great potential application values for detecting CP and the study is of great reference value for the research and development of biosensors for quantitative detection of organophosphate pesticides (OPs).

1. Introduction

Chlorpyrifos (CP) is one of the most widely used organophosphate pesticides (OPs) all over the world [1]. However, the accumulation of CP in farmland environment caused by excessive use of CP poses a serious health threat to human health and the environment [2]. Therefore, it is of great significance to develop a rapid, accurate and convenient method for detecting CP residues in agricultural products. Traditional CP detection methods including gas chromatography, high performance liquid chromatography and chromatography-mass spectrometry are time-consuming, expensive and need professional operations, seriously limiting the scope and field of their applications [3]. Electrochemical detection method based on biosensor has been widely studied in recent years due to its rapid, sensitive and convenient detection characteristics [1]. Many electrochemical detection platforms for OPs have been established, among which the acetylcholinesterase (AChE) based biosensor is the most extensively studied one with the best detection results [4]. However, the AChE based biosensors have to use Acetylthiocholine chloride (ATCl) as the electrochemical response substrate which greatly increases the biosensors' complexity [5]. Therefore, it is necessary to develop a novel OP biosensor based on other enzymes without substrate for simplicity purpose and improvement of biosensor performance.

There have been studies explored on the electrochemical properties of bovine hemoglobin (BHb) and designed BHb based biosensors for nitromethane (CH_3NO_2) determination [6]. An electrochemical biosensor based on BHb has been proposed to detect methyl parathion (MP) without using substrate showing good detection accuracy, stability and reliability [7]. BHb shows excellent application prospects in electrochemical biosensor design for its low cost, easy availability and good

* Corresponding author.
E-mail address: yybbao@sxau.edu.cn (H. Song).

https://doi.org/10.1016/j.enzmictec.2021.109959
Received 24 September 2021; Received in revised form 30 November 2021; Accepted 2 December 2021
Available online 3 December 2021

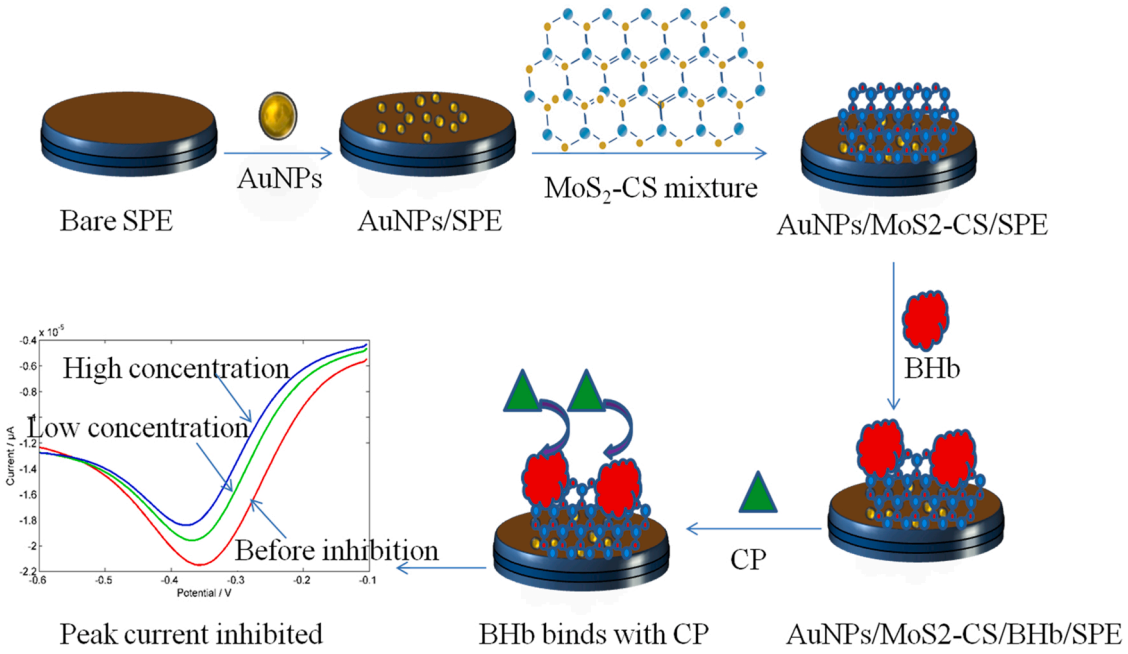

Scheme 1. Schematic illustration of the fabrication process and mechanism of the AuNPs/MoS_2-CS/BHb/SPE electrode.

biocompatibility [8]. For these reasons, a novel electrochemical biosensor based on BHb is proposed for detecting CP in this study.

In a previous study [9], the BHb based electrochemical biosensor shows two cathodic peak currents on the electrode surface at potential −0.8 V and −0.38 V respectively. The two cathodic peak currents are corresponding to two different reduction reactions: HbFe(III) to HbFe(II) and HbFe(II) to HbFe(I) respectively. The former reduction reaction was used for detecting nitromethane [6], and in the Indian research [7], the later reaction was used for determination of MP. Meanwhile, BHb could bind with CP and the process may form a thin film with poor conductivity hindering the electron transfer rate on the electrode surface [10]. This mechanism and principle was used to design a BHb based biosensor for determination of CP. The fabrication process and mechanism of the BHb based biosensor for CP assay is shown in Scheme 1.

2. Experimental

2.1. Reagents and instruments

Screen printed electrode (SPE) (TE100 3 mm/0.071 cm^2) was obtained from Zensor Research & Development company (Taiwan, China). Bovine hemoglobin (BHb) (lyophilized powder), phosphate buffer saline (PBS) and chitosan (CS) were obtained from COOLABER Technology Limited (Beijing China). Acetic acid (CH_3COOH), Potassium chloride (KCl), Calcium sulfate ($CaSO_4$), Sodium chloride (NaCl), Potassium ferricyanide ($K_3[Fe(CN)_6]$) and Potassium ferrocyanid ($K_4[Fe(CN)_6]$) were obtained from DAMAO CHEMICAL REAGENT FACTORY (Tianjin, China). Chlorpyrifos (CP) was obtained from Shanghai yongtuan Industrial Co., Ltd (Shanghai, China). Chloroauric acid ($AuCl_4H$) was obtained from Sigma-Aldrich (St. Louis, Mo, USA). Molybdenum disulfide (MoS_2) nanosheets were obtained from ZHEJIANG YAMEI NANO TECHNOLOGY CO. LTD (Hangzhou, China). The real samples of cabbage and leek were obtained from the local market. All the SPEs were ultrasonic cleaned in distilled water before use. All chemicals used in the experiments were of analytical purity.

Electrochemical studies were operated on a CHI760C electrochemical workstation (Shanghai CH instruments, China) at room temperature (25 ± 1 ℃). The surface morphological features of all prepared electrodes were investigated using the Field emission scanning electron microscopy (FESEM) (HITACHI S-4800) and HORIBA EMAX 7593-H along with energy dispersive X-ray spectroscopic analysis (EDS). All the electrochemical studies were performed in the three electrode systems with carbon electrode as working electrode (WE), carbon as counter electrode (CE) and Ag as the reference electrode (RE). All electrochemical experiments were carried out using the electrochemical software (chi760e.exe) with multichannel assembly. The square wave voltammetry (SWV) electrochemical technology was performed in PBS solution (pH 7) between the potential range of −0.1 V to −0.6 V with amplitude of + 0.25 V and frequency of 25 Hz. All experiment data processing was completed with MATLAB 2011b.

2.2. Fabrication of AuNPs modified SPE (AuNPs/SPE)

SPE was adopted to construct a portable and disposable biosensor for its small size, low price and high repeatability [11]. The surface of SPE was firstly modified with AuNPs through electrochemical deposition to increase the specific surface area and improve the conductivity, which contributed greatly to the super performance of the biosensor.

The specific operation steps are as follows: The bare SPE (carbon as WE) was treated using ultrasonic cleaning instrument with distilled water for 180 s before use [11]. To increase the specific surface area and conductivity of the SPE, a layer of gold nanoparticles was electrode positioned on the surface of the carbon working electrode to obtain AuNPs/SPE. Firstly 1% $AuCl_4H$ solution was prepared by dissolving 1 g of $AuCl_4H$ powder into 100 ml distilled water. Then the SPE was soaked into the 1% $AuCl_4H$ solution and treated with chronoamperometry method for 200 s (0.6 V, 25 Hz).

2.3. Fabrication of MoS_2-CS mixture modified SPE (AuNPs/MoS_2-CS/SPE)

Two-dimensional (2D) metal dichalcogenides MoS_2 as the analogue of graphene exhibits some outstanding properties such as ultrafast electronic conductivity, large surface area and ultrahigh electrocatalytic activity [12]. MoS_2 nanosheets show excellent performance in some electrochemical biosensors design and development. CS is a non-toxic biopolymer, which has unique biological regeneration, hydrophilicity, biodegradability, good film-forming property and large mechanical

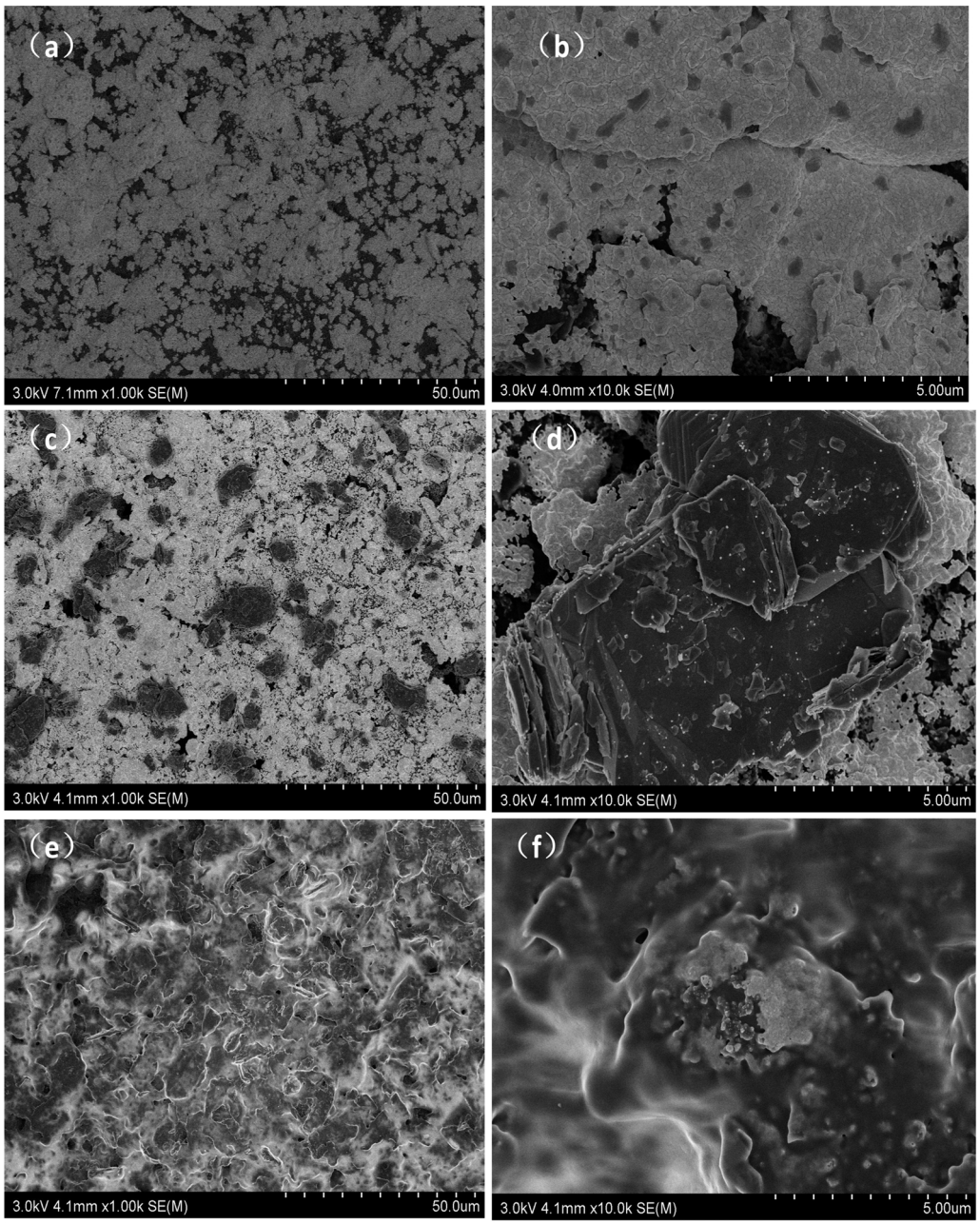

Fig. 1. FESEM images of (a) AuNPs/SPE at lower magnification and (b) at higher magnification (c) AuNPs/MoS_2-CS/SPE at lower magnification and (d) at higher magnification, (e) AuNPs/MoS_2-CS/BHb/SPE at lower magnification and (f) at higher magnification. (For interpretation of the references to colour in this figure, the reader is referred to the web version of this article.)

strength [13]. It is an environmentally friendly natural polymer that can gently and stably immobilize proteins and has been proved to be a suitable surface modifier for electrochemical biosensors [14]. Chitosan was often used in film entrapment to provide good biocompatible microenvironment for proteins (such as BHb), but the poor conductivity of CS hindered its application scope [15]. In our present work, MoS_2 nanosheets were blended with CS forming a mixed suspension to overcome this problem. The combination of MoS_2 nanosheets and CS (MoS_2-CS) could greatly enhance the conductivity of CS while maintaining its biocompatibility, which provides a good biological environment for BHb. The MoS_2-CS mixture suspension was then coated onto the SPE surface to further improve the conductivity and enhance the adsorption capacity of BHb.

The specific operation steps are as follows: 50 mg of MoS_2 nanosheets was added to 100 ml distilled water to obtain the MoS_2 suspension. The suspension was stirred for 3 min and then ultrasonic treated for 30 min. After that, 50 mg of CS was added into the MoS_2 suspension followed by ultrasonic treatment. Again, the mixed suspension was stirred for 3 min and then ultrasonic treated for 30 min to obtain the MoS_2-CS mixture suspension. Finally the MoS_2-CS mixture suspension was coated on AuNPs/SPE by dropping 10 μl of the mixed suspension onto the working electrode surface and left to dry at the room temperature (25 ± 1 ℃). With the simple drop coating method the SPE surface was then coated with a layer of MoS_2-CS mixture to obtain AuNPs/MoS_2-CS/SPE.

2.4. Immobilization of BHb on AuNPs/MoS_2-CS modified SPE (AuNPs/MoS_2-CS/BHb/SPE)

250 mg of BHb was added into 50 ml PBS solution (pH 7) to obtain

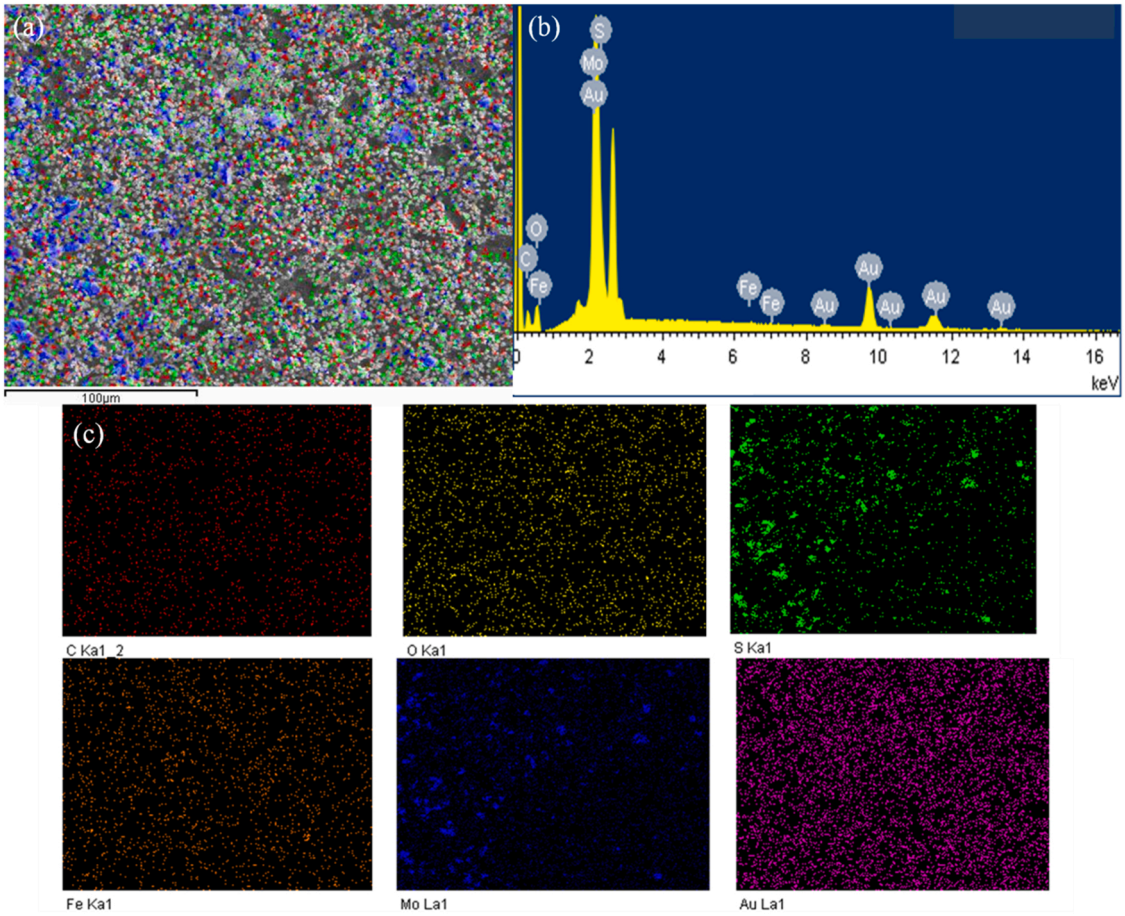

Fig. 2. (a) EDS spectra of AuNPs/MoS_2-CS/Hb/SPE, (b) elemental mapping of AuNPs/MoS_2-CS/Hb/SPE and (c) indicative of the element each color stands for.

the 5 mg ml^{-1} BHb solution. Drop casting 10 μl of the prepared BHb solution was done on the surface of AuNPs/MoS2-CS/SPE. Then the SPE was placed in ventilated and dry environment to naturally dry at room temperature (25 ± 1 ℃) to obtain AuNPs/MoS_2-CS/BHb/SPE. The obtained AuNPs/MoS_2-CS/BHb/SPE was finally thoroughly washed with PBS solution to remove the unbound BHb. The fabricated biosensors were stored in refrigerator at 4 ℃ for future use.

3. Results and discussions

3.1. Electrodes surface morphological studies

The SEM images of AuNPs/SPE, AuNPs/MoS_2-CS/SPE, and AuNPs/MoS_2-CS/BHb/SPE portrayed using FESEM were obtained to characterize the morphology of AuNPs and MoS_2 nano-materials on the surface of SPE. Fig. 1(a and b) represented the AuNPs/SPE SEM images at lower and higher magnification describing the gold nanoparticles morphology at the surface. It can be seen that a nearly uniform layer of gold nanoparticles is attached to the surface of the electrode illustrating the successful electrode position of the gold nanoparticles on the SPE surface. Fig. 1(c and d) represented the AuNPs/MoS_2-CS/SPE SEM images at lower and higher magnification depicting the nanosheets structure of MoS_2 and the uniformly distributed CS, which demonstrated the successful coating of MoS_2-CS mixture on AuNPs/SPE surface. Spherical molecule structure of BHb depicted in Fig. 1(e and f) demonstrated the successful immobilization of BHb due to the excellent film forming ability of CS to obtain AuNPs/MoS_2-CS/BHb/SPE. The BHb located on the outermost layer of the electrode surface was the core component and key substance of the proposed electrochemical biosensor. The nanomaterial (with good conductivity) modified SPE showing large specific surface area enabled large amount of BHb to load on the electrode surface.

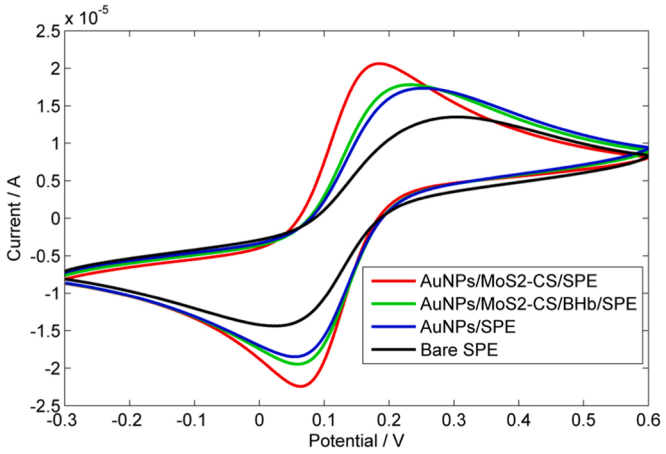

Fig. 3. CVs of bare SPE, AuNPs/SPE, AuNPs/MoS_2-CS/SPE, AuNPs/MoS_2-CS/BHb/SPE electrodes at scan rate of 25 mV s^{-1} using $[Fe(CN)_6]^{3-/4-}$ in KCl as redox probe.

The EDS spectra (Fig. 2) of AuNPs/MoS_2-CS/BHb/SPE proved the presence of Au, S, Mo, Fe, C and O elements which illustrated the successful coating of SPE with nanomaterials (AuNPs and MoS_2-CS) and the successful immobilization of BHb. SEM images and EDS spectra together showed the successful fabrication of the proposed electrochemical biosensor AuNPs/MoS_2-CS/BHb/SPE.

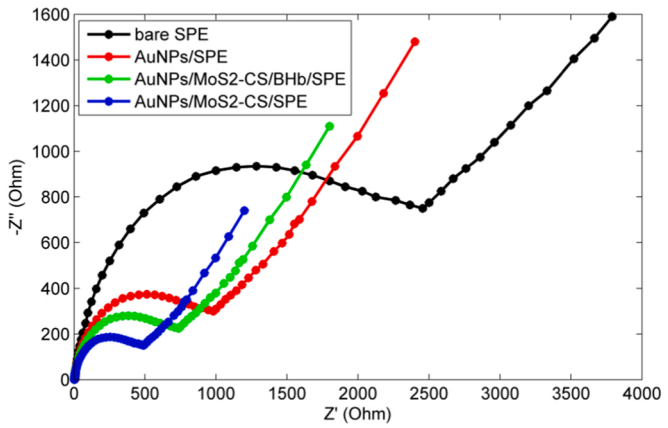

Fig. 4. Nyquist plots of bare SPE AuNPs/SPE, AuNPs/MoS_2-CS/SPE, and AuNPs/MoS_2-CS/BHb/SPE electrodes in 0.1 M KCl solution containing 0.1 mM $[Fe(CN)6]^{3-/4-}$.

3.2. Electrochemical studies of the electrodes

The electrochemical characteristics of all the prepared electrodes in the experimental section were tested with cyclic voltammetry (CV) technology (potential range between −0.3 V and +0.6 V) using 0.1 mM $[Fe(CN)_6]^{3-}$ and 0.1 mM $[Fe(CN)_6]^{4-}$ as redox couple in 0.1 M KCl solution at a scan rate of 25 mV s^{-1}. All CV curves showed a couple of typical well-defined reversible redox peaks relating to Fe^{3+}/Fe^{2+} redox. It can be seen from Fig. 3 in comparison with bare SPE electrode, after modification with AuNPs and MoS_2 nanosheets the peak current increased dramatically and the peak potential separation ΔE_p (the original value as 0.24 V) decreased which demonstrated the effectiveness of the electrode modification for improving the performance of the electrode. It was attributed to the good conductivity and large specific surface area of AuNPs and MoS_2 nanosheets that increase the electron transfer rate between electrode and redox probe. As shown in Fig. 3, the redox peak current was decreased after coating BHb on the AuNPs/MoS_2-CS/SPE electrode. This may be due to the weak conductivity of CS and BHb which hindered the electron's access to the surface of the electrode, and inhibited the electron transfer rate. Electrochemical characterization from another perspective confirmed the successful coating of AuNPs, MoS_2-CS, and BHb on the SPE surface.

3.3. Electrochemical impedance spectroscopy (EIS)

The EIS were tested on all fabricated electrodes with $[Fe(CN)_6]^{3-/4-}$ (0.1 mM) solution in KCl (0.1 M) as redox probe within the frequency range of 10^{-2}–10^5 Hz. The EIS of all electrodes Nyquist plots are depicted in Fig. 4. In all fabricated electrodes, EIS consists of a semicircle attribute to kinetically controlled phenomenon at higher frequencies and a straight line attribute to Warburg diffusion phenomenon at lower frequencies. The diameter of the semicircle indicative of electron-transfer resistance (R_{et}) reflecting the electron-transfer kinetics of the redox process at the electrodes surface decreased when the SPE was modified with AuNPs and MoS_2 nanosheets, whereas the R_{et} increased slightly after drop coating the electrodes with BHb. The results were consistent with previous CV tests illustrating that the nanomaterial modification improved the conductivity of SPE while BHb coating decreased the conductivity. The results indicated that AuNPs/MoS_2-CS nanomaterials could serve as an excellent transducer promoting electron transfer rate in electrochemical reactions which could greatly improve the performance of the biosensor. However, the conductivity of the biosensor decreased with the attachment of BHb on the electrode surface hindering the electron transfer rate. EIS tests proved the success of the nanomaterials and BHb modification from another aspect, indicating the successful fabrication of the electrochemical biosensor.

3.4. Optimization of the experimental parameters

To further improve the biosensor's performance, some critical parameters such as the mass ratio of MoS_2 nanaosheets and CS in their mixture suspension, the volume of BHb solution, the pH value of PBS solution, and the biosensor's incubation time with the pesticide were optimized through experiments. To optimize one parameter, all the other parameters were kept in optimal state.

The mass ratio of MoS_2 nanosheets and CS was an important

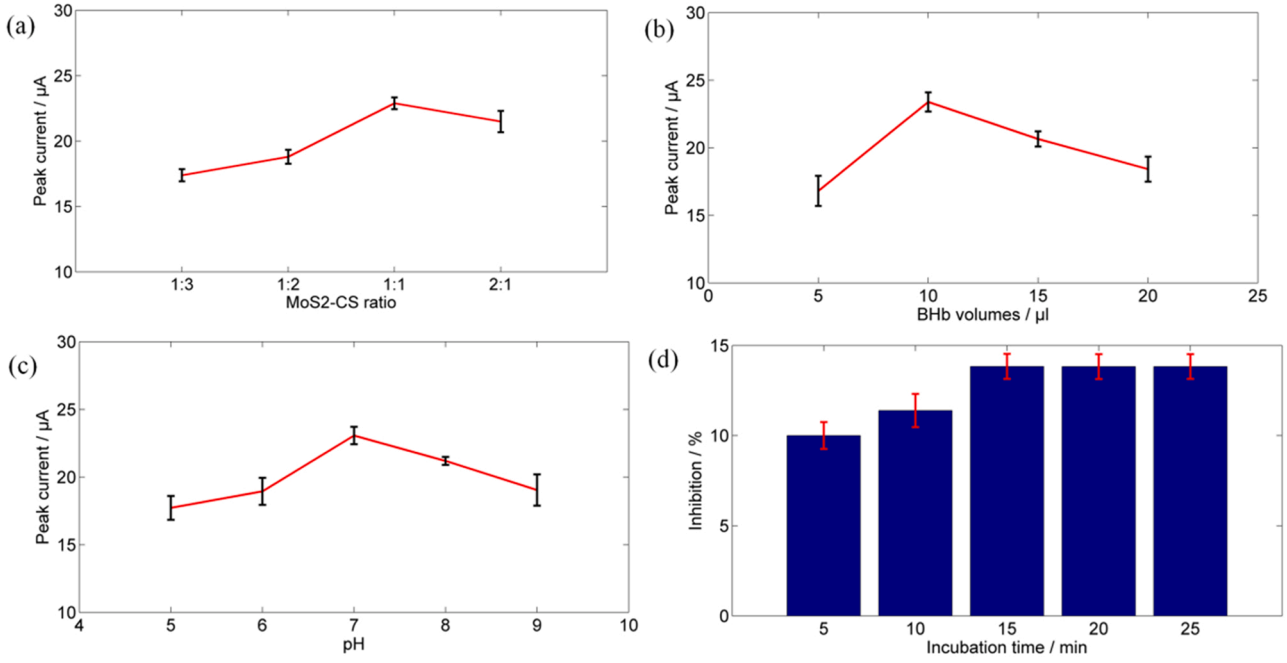

Fig. 5. Effect of (a) different MoS_2 -CS mass ratios, (b) different volumes of BHb (c) PBS pH value, and (d) incubation time on the responses of the proposed biosensor. Error bars are coefficient of variation across three repetitive experiments.

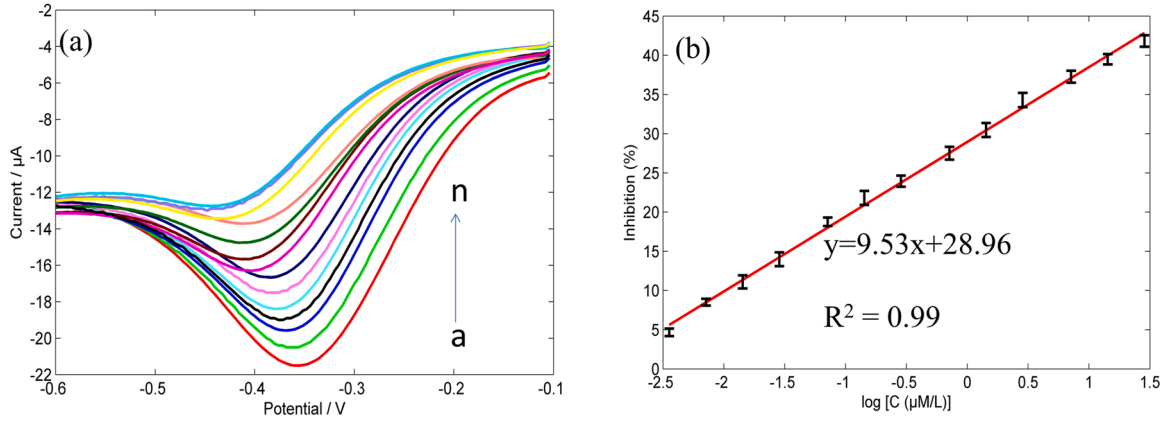

Fig. 6. SWV of AuNPs/MoS_2-CS/BHb/SPE in the presence of different concentrations of CP (a to n) (0–28.52 μM) , (b) calibration plot of peak current inhibition percent and logarithm of CP concentration between the linear range of 0.004 μM-28.52 μM.

parameter for the fabricated biosensor. The MoS_2 nanosheets serves as the super conductive material while the CS serves as a film entrapment material to absorb BHb. Only with suitable mass ratio can guarantee the biosensor with both good conductivity and adsorption capacity of BHb. Four different mass ratios (3:1, 2:1, 1:1 and 1:2) of MoS_2 nanosheets and CS mixture suspension were studied. It is obvious from Fig. 5(a) 1:1 ratio represent the optimal ratio, and in our present work we added 50 mg MoS_2 nanosheets and 50 mg CS (mass ratio 1:1) to 100 ml distilled water to obtain the MoS_2-CS mixture suspension.

The volume of BHb was also a very important parameter for the biosensor. Too little BHb could not evenly spread the surface of the working electrode, while too much BHb could easily overflow the working electrode surface leading to the leakage of BHb and the increase of the biosensor's impedance. Four different volumes (5 μl , 10 μl, 15 μl, 20 μl) of 5 mg ml^{-1} BHb solution were investigated through experiment. It can be seen from Fig. 5(b) that 10 μl of the BHb solution exhibited the maximum peak current and should be obtained as the optimal volume.

SWV response of the prepared biosensor was subjected to PBS electrolyte pH value change from 5 to 9. Both peak current and peak potential fluctuate with the change of pH values. With the increase of the pH value the peak potential moved toward left which was consistent with previous study [7]. To obtain the maximum peak current the neutral pH value 7 was selected as the optimal parameter in further electrochemical analysis (Fig. 5c).

It took a certain amount of time for BHb and CP to interact adequately with each other, and the time was considered as incubation time. Five different times (5 min, 10 min, 15 min, 20 min, 25 min) were investigated through experiment to optimize the incubation time. In Fig. 5(d), the peak current decreased (peak current inhibition percent increased) significantly with the increase of the incubation time within 15 min. However, when the incubation time exceeded 15 min the peak current stopped decreasing and kept steady. It demonstrated that the reaction of BHb and CP entered a saturated state after 15 min. To shorten the biosensor's detection process, 15 min was selected as the optimal incubation time in the following electrochemical analysis.

3.5. Mechanism analysis of the biosensor

The SWV is one of the most sensitive electrochemical techniques specifically when the analyte shows a fast electron transfer rate [16]. For this reason the SWV technology was adopted in this study. Electrochemical reactions of AuNPs/MoS_2-CS/BHb/SPE were monitored in 1 M PBS (pH 7) solution within the optimized conditions using the SWV technology. SWV responses with different CP concentrations were recorded and a cathodic peak current at potential −0.38 V was observed. The observed peak current was large due to the reduction reaction of BHbFe(III) to BHbFe(II). It was more likely to occur compared with the reduction reaction of BHbFe(II) to BHbFe(I) which usually occurred at a more negative potential (−0.8 to −1.2 V) [7,9]. The observed cathodic peak current was consistent with and confirmed by previous research [17].

SWV responses of different concentrations of CP were illustrated in Fig. 6(a). It can be seen that with the increase of CP concentration the peak current decreased as the electron transfer rate was hindered. The exact mechanism for the peak current inhibition appeared in the electrochemical system was not entirely clear. While we know that when CP was added to the electrolyte, it bound with BHb on the electrode surface [10]. The combination of BHb and CP on the surface of the electrode formed a thin film with poor conductivity. The thin film may block the electron transfer tunnel on the surface of the electrode, which contributed to the inhibition of the peak current. This may be the main reason for the inhibition of the electrochemical biosensor's peak current. The higher the concentration of CP added to the electrolyte, the more CP will combine with BHb on the electrode. The more CP combined with BHb, the thicker the film with poor conductivity formed. The thicker the film, the more obvious the inhibition of electron transfer rate, resulting in a stronger inhibition of the peak current. The corresponding relationship between the peak current inhibition percent and the concentration of CP can be used to accurately determinate the concentration of CP. The mechanism of the proposed electrochemical biosensor for detecting CP was shown in Scheme 1.

Suppose the blood protein BHb has *n* binding sites for the insecticide CP, and the cascade equilibria take place among BHb, CP and the complex as follows according to the study [10]:

$$BHb + nCP \leftrightarrow (CP)_n BHb$$

The existence of the combination $(CP)_nBHb$ directly inhibited the electron transfer tunnel, and the amount of the $(CP)_nBHb$ determined the peak current inhibition percent. While the number of BHb on the electrode surface was fixed (determined by the biosensor), so the number of $(CP)_nBHb$ was depended on the number of CP (that is, the concentration of CP). In this way, the inhibition percent of the peak current was directly related to the concentration of CP, and the principle could be used to determine the CP concentration.

The inhibition percent of the peak current can be calculated as follows:

$$inhibition(\%) = \frac{I_0 - I_1}{I_0} \times 100$$

Where I_0 is the peak current before inhibition (no CP added to the electrolyte) and I_1 is the peak current after inhibition (with CP added to the electrolyte) by the pesticide CP. Through the optimization experiments the incubation time was selected as 15 min, which means that it

Table 1
Comparison of different electrochemical biosensors developed for the detection of CP.

Electrode configuration	Linear range (μM)	LOD (nM)	References
AChE-[BMIM][BF4]-MWCNT/ CP	0.01–1	4	[18]
NA/Ag@rGO-NH2/ AChE/GCE	59.85–347.7	39.93	[19]
FTO-AuNPs	0.001–1	10	[20]
AChE/PB-CHIT/GCE	0.01–0.4	3	[21]
AuNPs/MoS_2-CS/BHb/SPE	0.004–28.52	5.6	Present work

took about 15 min for CP and BHb to adequately bind together to form the thin film.

According to the analysis above, the peak current inhibition percent increased with the CP concentration. As shown in Fig. 6(a), with the increase of CP concentration, the inhibition percent of peak current gradually increased until the CP concentration increased to a certain extent where maybe no more BHb to bind with CP. At this point, BHb could no longer bind with the excess CP added to the electrolyte, and the inhibition percent of peak current reached its peak. A linear calibration model was established between the inhibition percent (of the cathodic peak current) and the logarithm of the CP concentration (log C) over a range from 0.004 μM to 28.52 μM (Fig. 6b). The linear regression equation for the logarithm of CP concentration and the peak current inhibition percent is $Y = 9.53X + 28.96$, with a determination coefficient (R^2) of 0.99. The limit of detection (LOD) (with 3σ method, $\sigma = 2.5$) was 5.6 nM. In comparison with previous literature, the proposed biosensor in our present work show some advantages such as without using response substrate, a broader detection linear range and a relative lower LOD as shown in Table 1. In addition, the prepared biosensor used the disposable SPE which was inexpensive and ensured the consistency of the biosensor.

3.6. Repeatability, reproducibility, stability and anti-interference ability

Six successive SWV measurements using the AuNPs/MoS_2-CS/BHb/SPE were carried out to evaluate the repeatability of the proposed biosensor (Fig. 7a). The relative standard deviation (RSD) was 2.8% confirming the good repeatability of the proposed biosensor. For reproducibility, SWV technology was performed on six independent AuNPs/MoS_2-CS/BHb/SPE electrodes and the RSD obtained as 3.4% demonstrating the proposed biosensor with an appreciably reproducibility (Fig. 7b). The long term stability of the biosensor was investigated for 21 successive days (each investigation interval is 7 days), during which time the biosensors were kept in refrigerator at 4 °C. The BHb biological activity decreased and the protein denaturation occurred as the storage time prolonged. The SWV responses of the bioelectrodes were checked on day 7 and a 5.1% fall in peak current was observed. Moreover, 94.5% and 92.8% of the original peak current value was retained on day 14 and day 21 respectively. The results showed that the prepared biosensor exhibited good stability (Fig. 7c). To evaluate the anti-interference ability of the biosensor some electro-active interference substances such as Ca^{2+}, K^+, Cl^-, Na^+ were added to the electrolytic cell [11,22,23]. The experiment results showed that the presence of these interference substances have no significantly effect on the biosensor for determination of CP, which verifying the specificity of the BHb based biosensor (Fig. 7d). The results indicated that the prepared AuNPs/MoS_2-CS/BHb/SPE biosensor could selectively detect CP in the presence of these common interfering species commonly existed in agricultural products.

3.7. Real sample determination

To evaluate the authenticity of the proposed biosensor in real samples, cabbages and leeks obtained from the local market were made into real test samples as illustrated in Fig. 8. The leaves of cabbage and leek were thoroughly cleaned with distilled water and ground into paste with a mortar and pestle. The paste of the vegetable leaves was mixed thoroughly with PBS solution. The vegetable leaves paste mixed PBS solution was spiked with different concentrations of CP. Finally, the solution was centrifuged and the supernatant was collected. The supernatant containing CP pesticide residue was detected using the proposed electrochemical biosensor. Table 2 shows the recovery and RSD of different concentrations of CP in different real samples. The average recovery ranging from 87% to 109% have demonstrated the good applicability

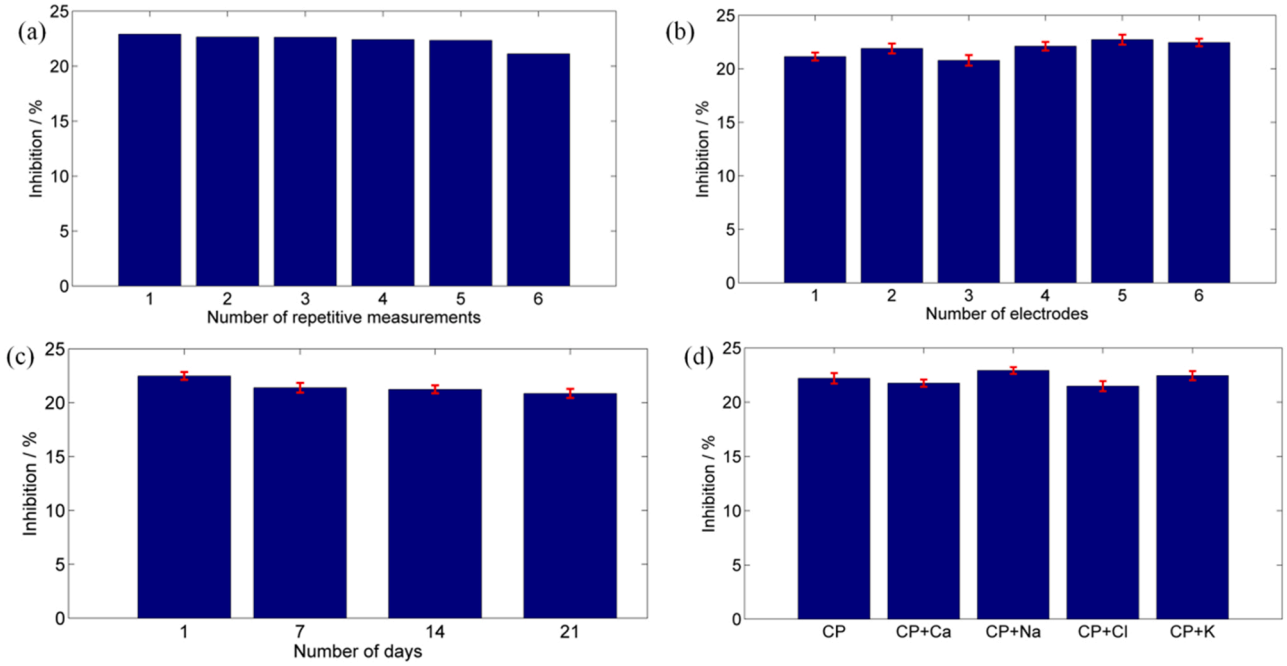

Fig. 7. SWV response of AuNPs/MoS_2-CS/BHb/SPE showing (a) evaluation of repeatability, (b) evaluation of reproducibility, (c) evaluation of stability and (d) evaluation of anti-interference ability in 0.143 μM of CP containing different analytes. Error bars are coefficient of variation across three repetitive experiments.

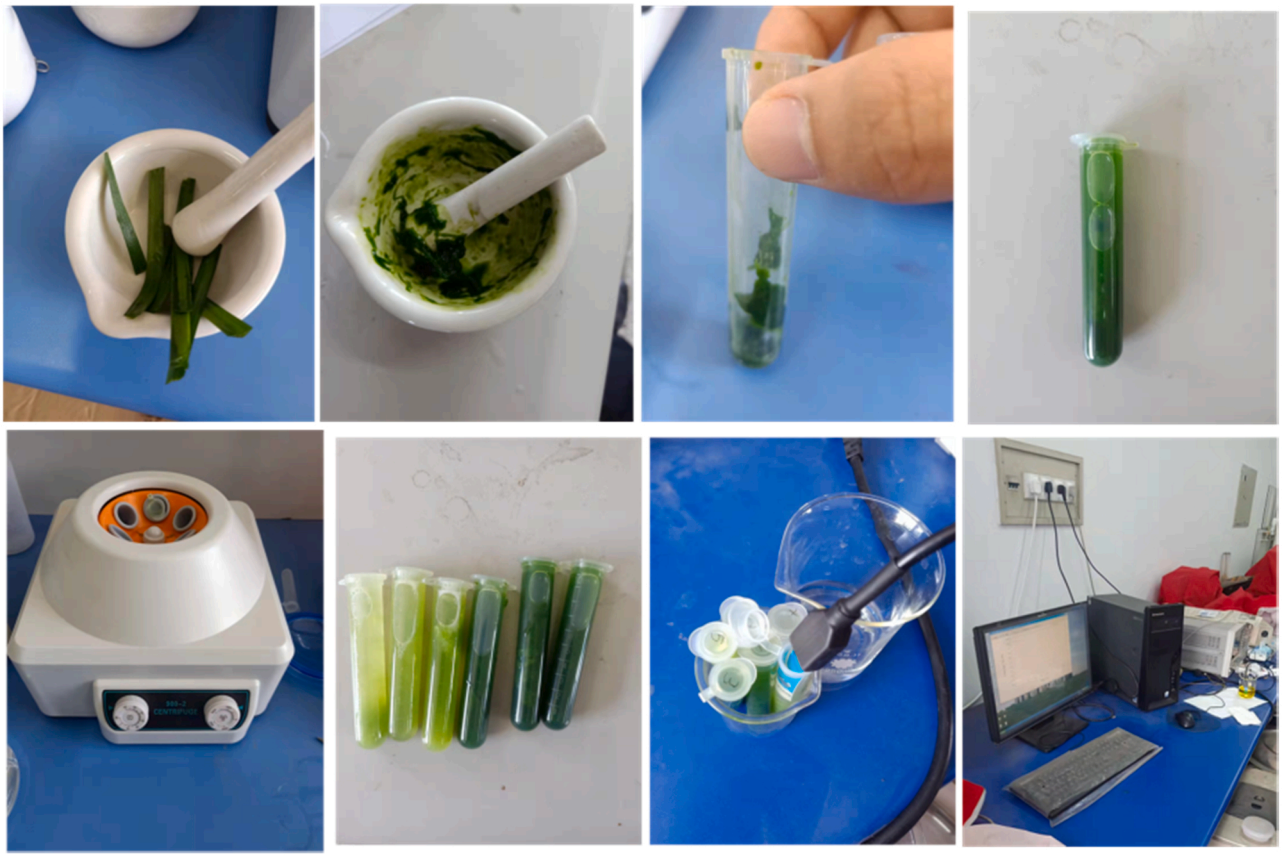

Fig. 8. The detection process of pesticide residues in real vegetable samples.

Table 2
Recovery test of chlorpyrifos in cabbage and leek samples.

Samples	Spiked levels (μM)	Calculated value (μM)	Recovery %	RSD (%, n = 3)
Cabbage	0.029	0.025	87.36	6.03
	0.285	0.308	107.95	1.90
	2.852	3.116	109.24	0.82
Leek	0.029	0.026	88.51	2.25
	0.285	0.302	106.08	4.04
	2.852	3.041	106.63	2.34

and authenticity of the prepared AuNPs/MoS_2-CS/BHb/SPE biosensor in complex real vegetable samples [11,24].

4. Conclusions

This study reports the development of a novel BHb based disposable biosensor AuNPs/MoS_2-CS/BHb/SPE for quantitative determination of CP. BHb binds with CP at the bioelectrode surface forming a thin film with poor conductivity which hinders the electron transfer tunnel and inhibits the electron transfer rate. In this way the peak current is inhibited on the surface of the bioelectrode. We have cleverly used this mechanism to design the AuNPs/MoS_2-CS/BHb/SPE bioelectrode. Compared with the traditional AChE based electrochemical biosensor for OPs detection, the proposed biosensor does not need reaction substrate, which not only simplifies the fabrication process but also increases the whole performance of the biosensor. The present biosensor exhibits good performance for detecting CP with a broad linear range of 0.004 μM to 28.52 μM, and the LOD as 5.6 nM. Reliable experiments have verified the repeatability, reproducibility, stability and anti-interference ability of the biosensor. Real vegetable samples tests monitoring CP show good results with recovery (%) from 87% to 109%. The proposed biosensor exhibits some advantages such as high sensitivity and stability, simple fabrication and low cost. It is broadly applicable and highly prospective for future CP pesticide residues detection.

CRediT authorship contribution statement

Wei Li: Conceptualization, Methodology, Formal analysis, Software, Writing – original draft, Writing – review & editing, Validation, Resources. **Zuyi Zhao:** Resources, Investigation, Software. **Wei Yang:** Resources, Data curation, Software. **Qin Su:** Resources, Investigation. **Na Chong:** Investigation. **Xueli Zhang:** Investigation. **Rui Zhao:** Investigation. **Haiyan Song:** Conceptualization, Methodology, Funding acquisition, Project administration, Supervision.

Acknowledgements

This work was funded by the National Key Research and Development Program of China (No. 2018YFD0700300).

References

[1] S. Uniyal, R.K. Sharma, Technological advancement in electrochemical biosensor based detection of Organophosphate pesticide chlorpyrifos in the environment: a review of status and prospects, Biosens. Bioelectron. 116 (2018) 37–50.
[2] J. del Pino, P. Moyano, M.J. Anadon, J.M. García, M.J. Díaz, G. Gómez, J. García, M.T. Frejo, SN56 basal forebrain cholinergic neuronal loss after acute and long-term chlorpyrifos exposure through oxidative stress generation; P75NTR and α7-nAChRs alterations mediated partially by AChE variants disruption, Toxicology 353-354 (2016) 48–57.
[3] L.C. Schrübbers, M. Masís-Mora, E. Carazo Rojas, B.E. Valverde, J.H. Christensen, N. Cedergreen, Analysis of glyphosate and aminomethylphosphonic acid in leaves from Coffea arabica using high performance liquid chromatography with quadrupole mass spectrometry detection, Talanta 146 (2016) 609–620.

[4] S. Rana, R. Kaur, R. Jain, N. Prabhakar, Ionic liquid assisted growth of poly(3,4-ethylenedioxythiophene)/reduced graphene oxide based electrode: an improved electro-catalytic performance for the detection of organophosphorus pesticides in beverages, Arab. J. Chem. 12 (7) (2019) 1121–1133.
[5] N. Chauhan, J. Narang, C.S. Pundir, Immobilization of rat brain acetylcholinesterase on ZnS and poly(indole-5-carboxylic acid) modified Au electrode for detection of organophosphorus insecticides, Biosens. Bioelectron. 29 (1) (2011) 82–88.
[6] Y. Wen, W. Wen, X. Zhang, S. Wang, Highly sensitive amperometric biosensor based on electrochemically-reduced graphene oxide-chitosan/hemoglobin nanocomposite for nitromethane determination, Biosens. Bioelectron. 79 (2016) 894–900.
[7] R. Kaur, S. Rana, K. Lalit, P. Singh, K. Kaur, Electrochemical detection of methyl parathion via a novel biosensor tailored on highly biocompatible electrochemically reduced graphene oxide-chitosan-hemoglobin coatings, Biosens. Bioelectron. 167 (2020), 112486.
[8] Y. Wang, H. Xiong, X. Zhang, Y. Ye, S. Wang, Nitromethane biosensor based on four heme proteins modified glassy carbon electrodes, J. Electroanal. Chem. 674 (2012) 17–22.
[9] N. Jović-Jovičić, Z. Mojović, M. Mojović, P. Banković, M. Ajduković, A. Milutinović-Nikolić, D. Jovanović, Electrochemical behavior of immobilized hemoglobin in alkaline solution, Appl. Surf. Sci. 400 (2017) 347–354.
[10] Y. Cui, J. Guo, B. Xu, Z. Chen, Binding of chlorpyrifos and cypermethrin to blood proteins, Pestic. Biochem. Physiol. 85 (2) (2006) 110–114.
[11] F. Zhao, Y. Yao, X. Li, L. Lan, C. Jiang, J. Ping, Metallic transition metal dichalcogenide nanosheets as an effective and biocompatible transducer for electrochemical detection of pesticide, Anal. Chem. 90 (19) (2018) 11658–11664.
[12] Q. Qiu, H. Chen, S. Sharif, Z. You, S. Ying, Y. Wang, Y. Ying, Ultrathin noble metal nanoplates decorated metal-organic framework nanosheets as 2D/2D heterojunction nanobionic catalysts for explosive residues monitoring, 2D Mater. 6 (3) (2019), 035008.
[13] L. Wang, Y. Zhang, A. Wu, G. Wei, Designed graphene-peptide nanocomposites for biosensor applications: a review, Anal. Chim. Acta 985 (2017) 24–40.
[14] W. Suginta, P. Khunkaewla, A. Schulte, Electrochemical biosensor applications of polysaccharides chitin and chitosan, Chem. Rev. 113 (7) (2013) 5458–5479.
[15] A. Baranwal, A. Kumar, A. Priyadharshini, G.S. Oggu, I. Bhatnagar, A. Srivastava, P. Chandra, Chitosan: an undisputed bio-fabrication material for tissue engineering and bio-sensing applications, Int. J. Biol. Macromol. 110 (2018) 110–123.
[16] F. Garay, S.N. Vettorelo, How to obtain kinetic information in thin-film voltammetry from the comparison of SCV and SWV responses, J. Electroanal. Chem. 878 (2020), 114647.
[17] H.-H. Liu, G.-L. Zou, Electrochemical investigation of immobilized hemoglobin: redox chemistry and enzymatic catalysis, J. Biochem. Biophys. Methods 68 (2) (2006) 87–99.
[18] L.-G. Zamfir, L. Rotariu, C. Bala, A novel, sensitive, reusable and low potential acetylcholinesterase biosensor for chlorpyrifos based on 1-butyl-3-methylimidazolium tetrafluoroborate/multiwalled carbon nanotubes gel, Biosens. Bioelectron. 26 (8) (2011) 3692–3695.
[19] M. Guler, V. Turkoglu, Z. Basi, Determination of malation, methidathion, and chlorpyrifos ethyl pesticides using acetylcholinesterase biosensor based on Nafion/Ag@rGO-NH_2 nanocomposites, Electrochim. Acta 240 (2017) 129–135.
[20] A. Talan, A. Mishra, S.A. Eremin, J. Narang, A. Kumar, S. Gandhi, Ultrasensitive electrochemical immuno-sensing platform based on gold nanoparticles triggering chlorpyrifos detection in fruits and vegetables, Biosens. Bioelectron. 105 (2018) 14–21.
[21] Y. Song, M. Zhang, L. Wang, L. Wan, X. Xiao, S. Ye, J. Wang, A novel biosensor based on acetylecholinesterase/prussian blue–chitosan modified electrode for detection of carbaryl pesticides, Electrochim. Acta 56 (21) (2011) 7267–7271.
[22] X. Lu, L. Tao, D. Song, Y. Li, F. Gao, Bimetallic Pd@Au nanorods based ultrasensitive acetylcholinesterase biosensor for determination of organophosphate pesticides, Sens. Actuators B Chem. 255 (2018) 2575–2581.
[23] D. Song, Q. Li, X. Lu, Y. Li, Y. Li, Y. Wang, F. Gao, Ultra-thin bimetallic alloy nanowires with porous architecture/monolayer MoS2 nanosheet as a highly sensitive platform for the electrochemical assay of hazardous omethoate pollutant, J. Hazard. Mater. 357 (2018) 466–474.
[24] Communities, Official Journal of the European Communities (2002) Commission Decision of 12 August 2002 Implementing Council Directive 96/23/EC Concerning the Performance of Analytical Methods and the Interpretation of Results., Official Journal of the European Union, 2002, pp. L221–L228.